CHAPTER IV

RESULTS AND DISCUSSION

1. Extraction of RBO

1.1. The Effect of Production Methods on Oil Quality

The quality of RBO was affected by the method of extraction. Figure 22 showed colors of RBO extracted by different production methods when comparing with RE-RBO. RE-RBO gave less color compared to the RBO produced by SE, BSE, CP and BCP production methods.

The CP gave less color than SE, which yielded dark yellow color. The color of SE-RBO and CP-RBO were changed to light color by bleaching process using activated charcoal. BCP-RBO gave less color when compare to CP-RBO. Also, the BSE-RBO gave less color than SE-RBO. The results were summarized in Table 6. These results confirm that the RBO quality (color) depending upon the various production methods (Kochhar, 2002). The percent yields (Table 7) of BSE-RBO and BCP-RBO from bleaching processed were 72.72 and 73.51% (w/w), respectively

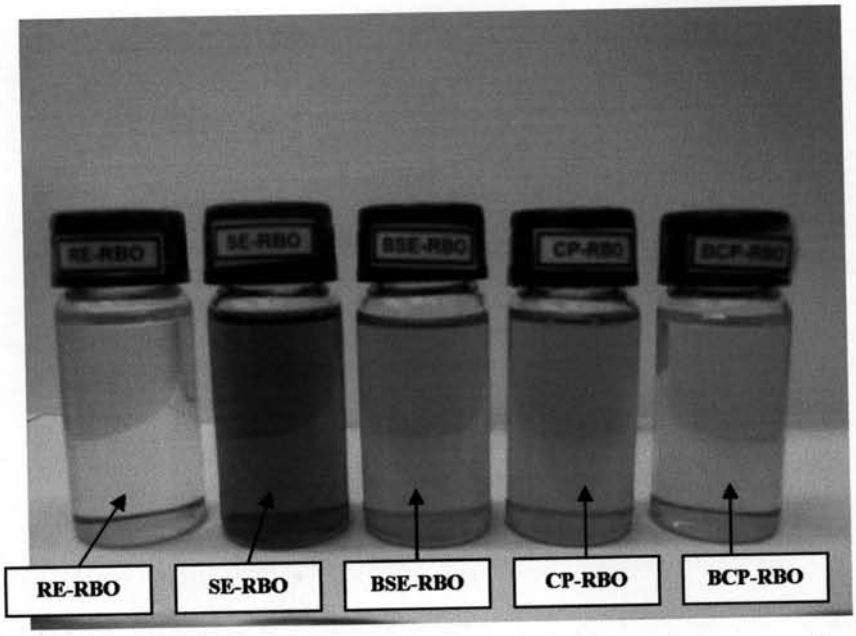

Figure 22 Samples of RBO produced by different methods compared to commercial RBO (RE-RBO)

Table 6 Color of various production methods

Production method	Color
SE-RBO	+++++
BSE-RBO	++++
CP-RBO	++++
BCP-RBO	++
RE-RBO	+

Visual estimation: + = light yellow color, ++ = yellow color, ++++ = dark yellow color, +++++ = dark brown color

Table 7 The percent yield of BSE-RBO and BCP-RBO from bleaching step.

RBO	% yield (w/w)
BSE-RBO	72.73±0.78
BCP-RBO	73.52±1.06

Mean ± S.D. (n=3)
%yield = (RBO before bleached –RBO after bleached) x 100/RBO before bleached

1.2. Viscosity of RBO from Various Production Methods

The estimated viscosity can be ranked from the lowest to highest, as follows: RE-RBO (90.81 ± 0.60), BCP (90.97 ± 0.24), CP-RBO (90.99 ± 0.43), BSE-RBO (91.73 ± 0.52), and SE-RBO (92.01 ± 0.75) were shown in Figure 23.

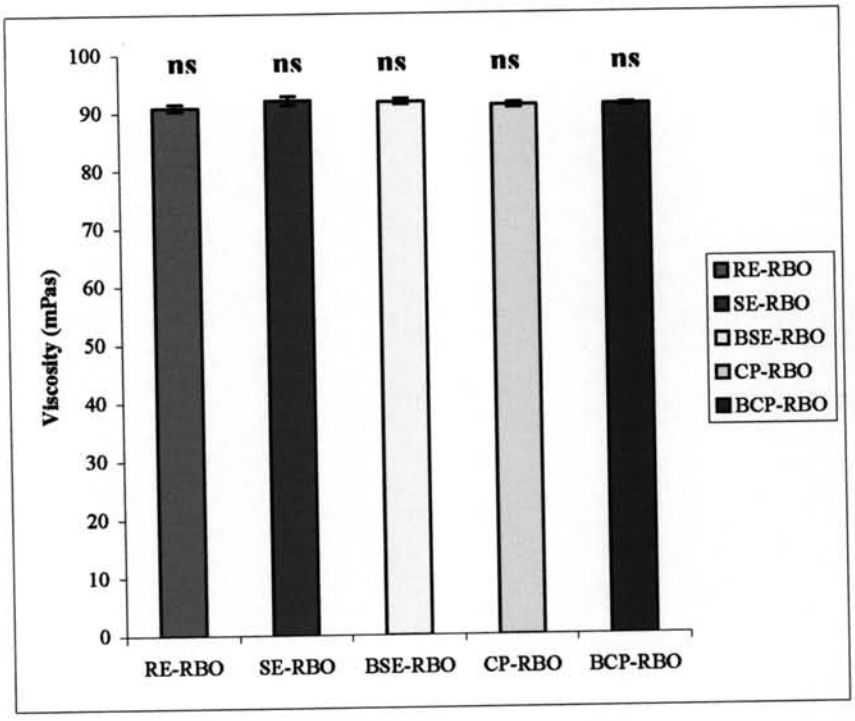

Figure 23 Viscosities of RBO from various RBO
(Each bar represent mean ± SD, ns = no significant difference Between group (P>0.05))

The difference in term of pH for the RBO from various production methods were not significant (P>0.05).

2. Determination of Antioxidant Activity of Various RBO

2.1. Hydrogen-donating Activity (DPPH radical scavenging activity)

Antioxidant activity was determined by the interaction of the sample with DPPH, either transferring an electron or hydrogen atom to DPPH·, and thus neutralizing its free radical character. The resultant color was changed from purple to yellow which was assessed by measuring sample absorbance at 517 nm, then was evaluated by comparison with control sample without hydrogen donating ability of the test compounds. The percent inhibitions of the test samples of RBO from various production methods were calculated and the results were plotted against concentrations as shown in Figure 24. From the plot of percentage of DPPH scavenging activity (% inhibition of free radical) against concentrations (0, 1, 2, 4, 5, 6, 8, 10, 12 and 16 mg/mL) of test samples.

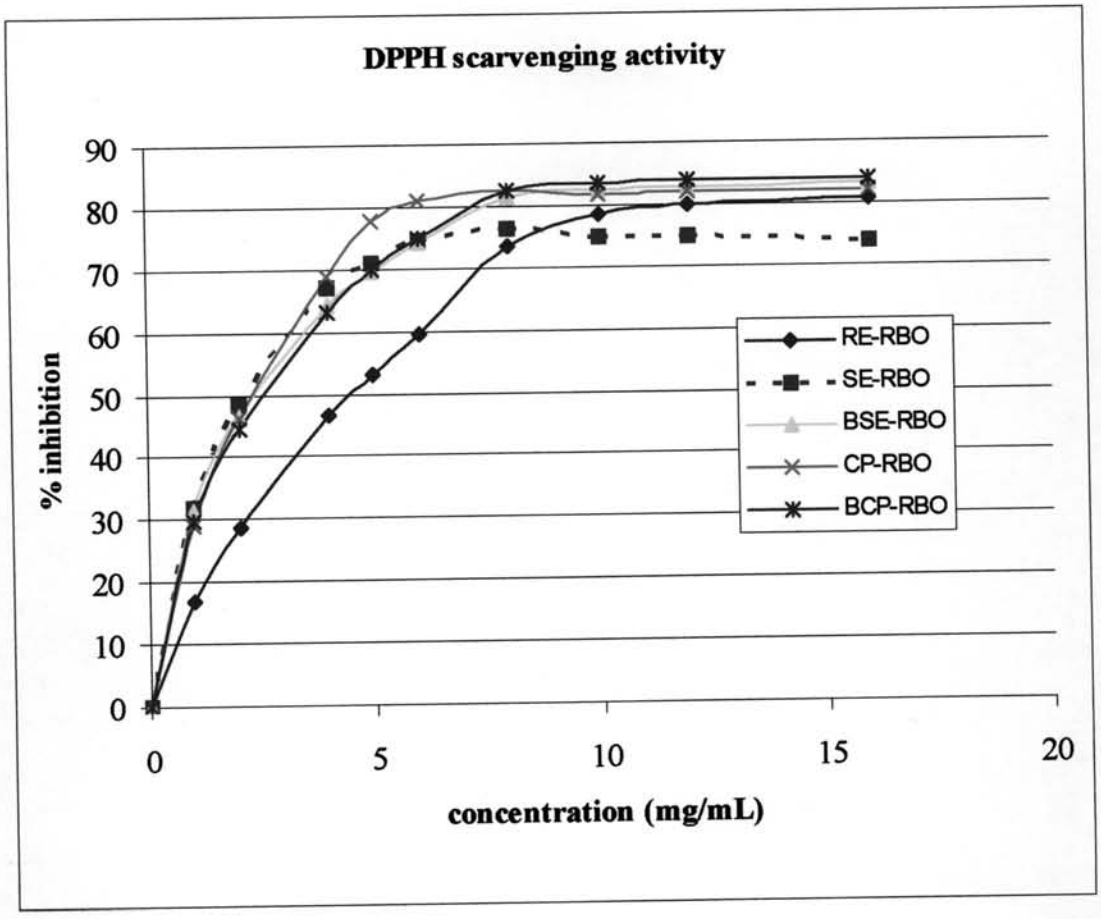

Figure 24 DPPH radical inhibition of various RBO (Mean ± SD, n = 3).

SE-RBO was found to exhibit the highest DPPH scavenging activity followed by CP-RBO, BSE –RBO, BCP-RBO and RE-RBO. This indicated that the radical scavenging activity of antioxidant was decreased with increasing production steps.

Figure 24 demonstrated the percent DPPH radical inhibition of 77.33 ± 0.65, 81.26 ± 1.44, 83.45 ± 1.54, 82.69 ± 1.80, 73.90 ± 1.50 at 8.00 mg/mL of SE-RBO, BSE-RBO, CP-RBO BCP-RBO and RE-RBO, respectively.

The concentration at 50 % inhibition (IC_{50}) of each sample was calculated from the equation of partial polynomial plot as shown in Table 8.The estimated IC_{50} can be ranked from the lowest to highest, as follows: SE-RBO (2.23 mg/mL± 0.22), CP-RBO (2.29 mg/mL ± 0.04), BSE-RBO (2.46 mg/mL ± 0.21), BCP-RBO (2.59 ± 0.14) and RE-RBO (4.53 mg/mL ± 0.12); Since the lower IC_{50} value gave the greater scavenging potency of the antioxidant, therefore, SE-RBO present the highest DPPH

radical scavenging activity, followed by CP-RBO, BSE-RBO, BCP-RBO and RE-RBO.

Table 8 The IC_{50} value for DPPH radical scavenging activity of each various production methods of RBO

Sample	Polynomial equation			
	IC50 (mg/mL)	Mean (mg/mL)	SD	R^2
RE-RBO	4.42	4.53	0.12	0.9989
	4.65			0.9982
	4.53			0.9989
SE-RBO	1.98	2.23	0.22	0.9927
	2.32			0.9966
	2.38			0.9972
BSE-RBO	2.32	2.46	0.21	0.9945
	2.35			0.9994
	2.70			0.996
CP-RBO	2.30	2.29	0.04	0.9979
	2.25			0.9968
	2.32			0.9995
BCP-RBO	2.50	2.59	0.14	0.9976
	2.53			0.9984
	2.75			0.9943

(Mean ± S.D., n=3)

From Figure 25 bleaching process (BSE-RBO and BCP-RBO) showed that their DPPH scavenging activity was lower than non-bleaching oil (SE-RBO and CP-RBO). Moreover, the DPPH scavenging activity of the RE-RBO showed the lowest activity.

The IC_{50} data were subsequently analyzed by one-way analysis of variance (ANOVA) at 95 % confidence level followed by Tukey's test. There were no significant differences in antioxidant among SE-RBO, BSE-RBO, CP-RBO and BCP-RBO except for RE-RBO, which was significant ($P<0.05$).

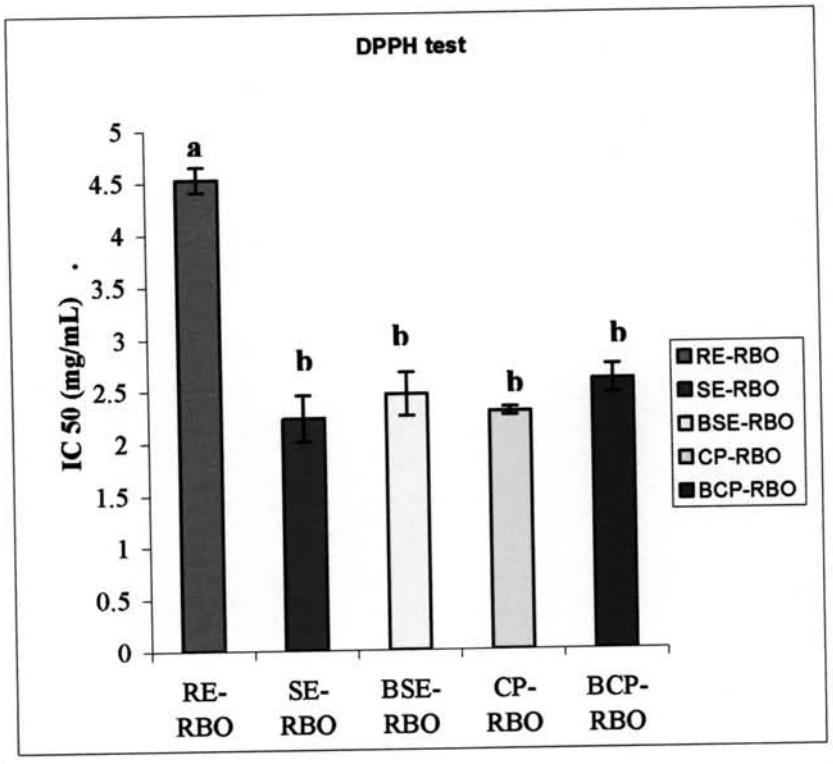

Figure 25 The IC_{50} (mg/mL) of various production methods for DPPH radical inhibition (Each bar represent mean ± SD, n = 3, a, b = significant difference between group ($P<0.05$))

These results indicated that the DPPH radical inhibition ability of RE-RBO showed the lowest among production methods. This might be due to several passing through processing steps of RE-RBO. Each step of processing could be reduced the content of antioxidant in RBO.

Additionally, the radical-scavenging activity was found in 5 production methods might be according to the content of γ-oryzanol and α-tocopherol (Sayre, 1988). These results will lead to the conclusion that γ-oryzanol and α-tocopherol are main antioxidant in RBO. The content of γ-oryzanol and α-tocopherol were analyzed by HPLC in further study (3.2 and 3.3).

3. Determination of γ-Oryzanol and Vitamin E (α-tocopherol) content in Various RBO

3.1 HPLC Method Validation of γ-Oryzanol

The standard preparations were carried out in triplicate at each concentration. Then, the prepared working standard solutions were analyzed by HPLC. The peak area and stand curve of γ-oryzanol were shown in Table 9 and Figure 26.

Table 9 Peak area of γ-oryzanol standard (standard curve)

Sample	Conc. (mg/mL)	Peak Area
		γ-oryzanol
Std 1	0.0099	234244.3
Std 2	0.0247	683108.7
Std 3	0.0495	1538332
Std 4	0.0990	2768066
Std 5	0.2474	7626621
Std 6	0.4948	15132678

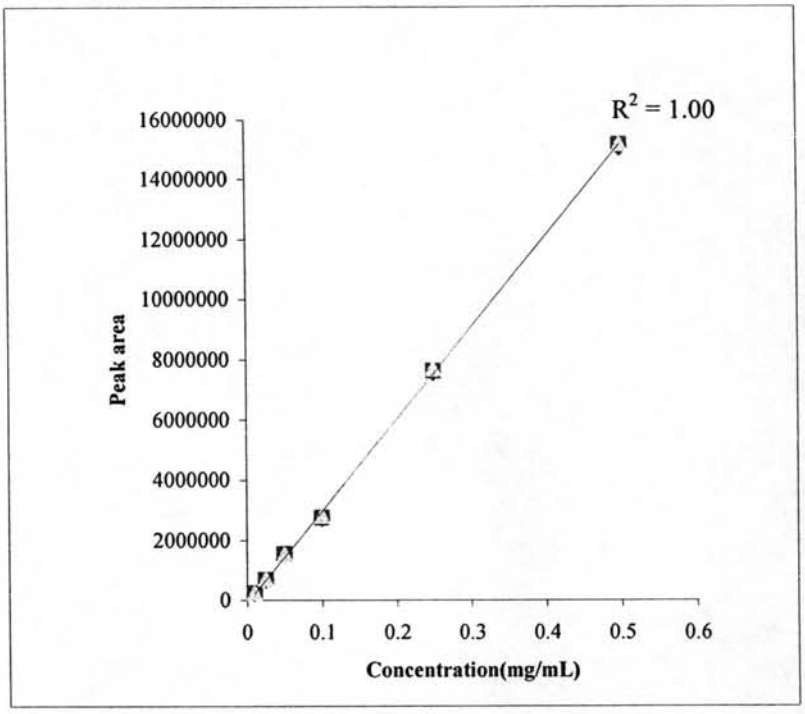

Figure 26 Standard curve of γ-oryzanol

3.1.1 Accuracy

Accuracy study of analytical method of γ-oryzanol at tree concentrations were carried out. The results were shown in Table 10.

From the accuracy results of γ-oryzanol in Table 10 at concentration of 0.0247, 0.0495 and 0.0990 mg/mL provided the average of 99.44%, 98.65%, and 98.83 %, respectively. The relative standard deviation percentages (%RSD) of individual concentration were 1.64%, 1.39 %, and 0.93%. The percent recoveries were in the range of 98-102%

3.1.2 Precision

The determination of precision of the method for the assay of γ-oryzanol was performed with six replicated sample solutions with out a serial dilution at 0.0495 mg/mL of the test concentration.

According to the results of intra-day of γ-oryzanol as shown in Table 11, the %recoveries were between 98.87 % and 101.71 % with an average of 100.13 %. The %RSD was 1.18 %. Table 12 showed inter-day precision; the %recoveries of day 1, 2, and 3 were 100.13%, 100.85 %, and 99.86 %, respectively.

3.1.3 Linearity and Range

The linearity of the method was studied at tree different concentrations of sample solution (0.0247, 0.0495 and 0.0990 mg/mL of the test concentration) without a serial dilution. The selected concentrations covered the ranges of each analyte in all test samples. The results were shown in Table 13. The graph of each component (Figure 27) obtained by plotting the observed concentration against the actual concentration was a straight line with R^2 of γ-oryzanol was 1.000.

Table 13 and figure 27 showed that, at γ-oryzanol concentration of 0.0247, 0.0495 and 0.0990 mg/mL, The actual concentrations and the observed concentration provided the linear relationship with linear equation $y = 0.9818x+0.0006$ and $R^2 \geq 1.000$

Table 10 Accuracy of γ-oryzanol

Sample ID	Actual conc. (mg/mL)	Observed conc. (mg/mL)	% Recovery	Average (Range)	% RSD
1A	0.0247	0.0244	98.53	100.26 (98.53-101.81)	1.64
1B	0.0247	0.0249	100.46		
1C	0.0247	0.0252	101.81		
2A	0.0495	0.0491	99.23	99.84 (98.87-101.44)	1.39
2B	0.0495	0.0489	98.87		
2C	0.0495	0.0502	101.44		
3A	0.0990	0.0988	99.87	98.83 (98.16-99.87)	0.93
3B	0.0990	0.0974	98.46		
3C	0.0990	0.0971	98.16		

Table 11 Intra-day precision of γ-oryzanol

Sample ID	Actual conc. (mg/mL)	Observed conc. (mg/mL)	% Recovery	Average (Range)	% RSD
2A	0.0495	0.0491	99.23	100.13 (98.87-101.71)	1.18
2 B	0.0495	0.0489	98.87		
2C	0.0495	0.0502	101.44		
2D	0.0495	0.0492	99.50		
2E	0.0495	0.0495	100.06		
2F	0.0495	0.0503	101.71		

Table 12 Inter-day precision of γ-oryzanol

Day	Sample ID	Actual conc. (mg/mL)	Observed conc. (mg/mL)	% Recovery	Average (Range)	% RSD
1	*2A*	0.0495	0.0491	99.23	100.13	1.18
	2 B	0.0495	0.0489	98.87		
	2C	0.0495	0.0502	101.44		
	2D	0.0495	0.0492	99.50		
	2E	0.0495	0.0495	100.06		
	2F	0.0495	0.0503	101.71		
2	*2A*	0.0495	0.0504	101.86	100.85	0.92
	2 B	0.0495	0.0501	101.15		
	2C	0.0495	0.0492	99.41		
	2D	0.0495	0.0496	100.31		
	2E	0.0495	0.0497	100.46		
	2F	0.0495	0.0504	101.91		
3	*2A*	0.0495	0.0498	100.64	99.56	1.21
	2 B	0.0495	0.0485	98.06		
	2C	0.0495	0.0501	101.23		
	2D	0.0495	0.0490	99.09		
	2E	0.0495	0.0488	98.64		
	2F	0.0495	0.0493	99.68		

Table 13 Linearity of γ-oryzanol

Sample ID	Actual conc. (mg/mL)	Average actual conc.(mg/mL)	Observed conc. (mg/mL)	Average observed conc.(mg/mL)
1A	0.0247	0.0247	0.0244	0.0248
1B	0.0247		0.0249	
1C	0.0247		0.0252	
2A	0.0495	0.0495	0.0491	0.0494
2B	0.0495		0.0489	
2C	0.0495		0.0502	
3A	0.0990	0.0990	0.0988	0.0978
3B	0.0990		0.0974	
3C	0.0990		0.0971	

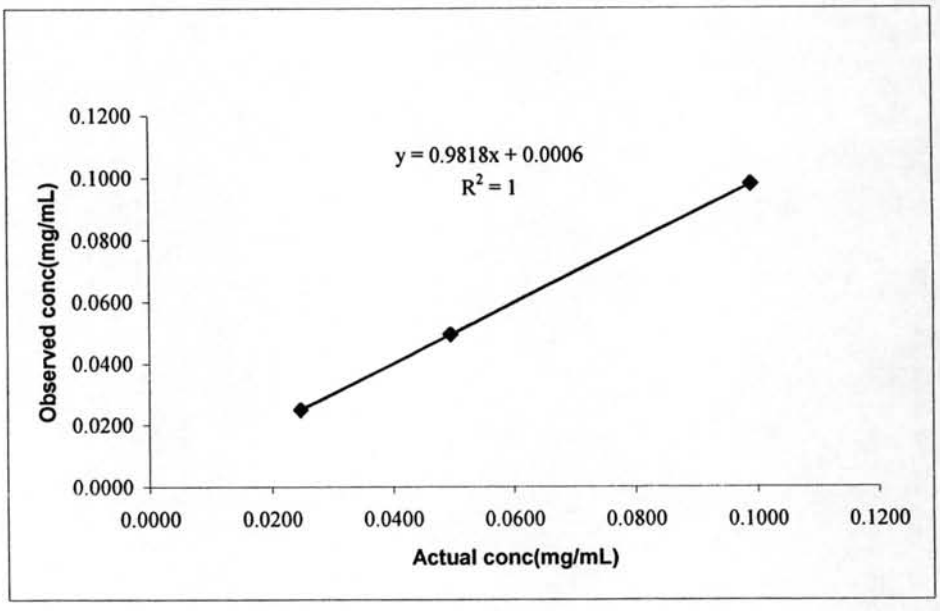

Figure 27 Linearity graph of γ-oryzanol

3.1.4 Selectivity

Selectivity of the analytical method was investigated by injection standard solution of γ-oryzanol and then comparing chromatograms of diluting solution.

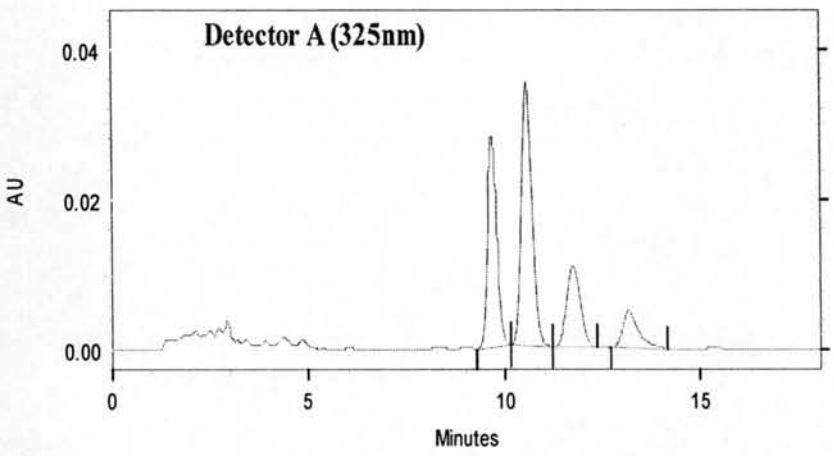

Figure 28 Chromatogram of γ-oryzanol standard

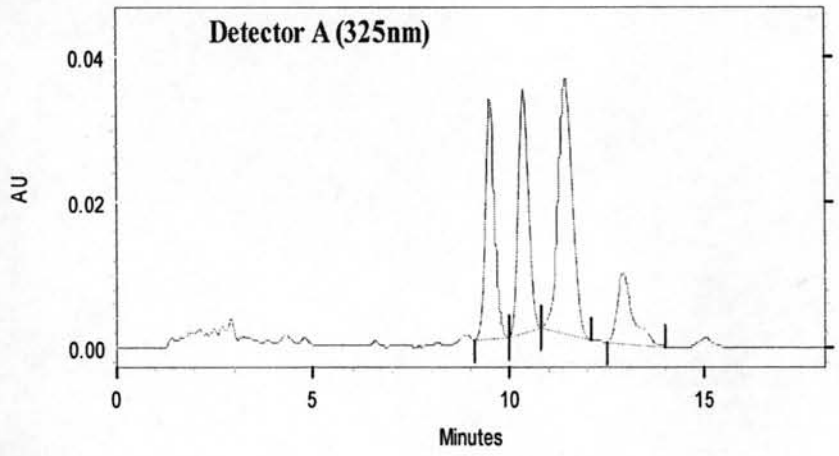

Figure 29 Chromatogram of 10% w/v C-RBO sample

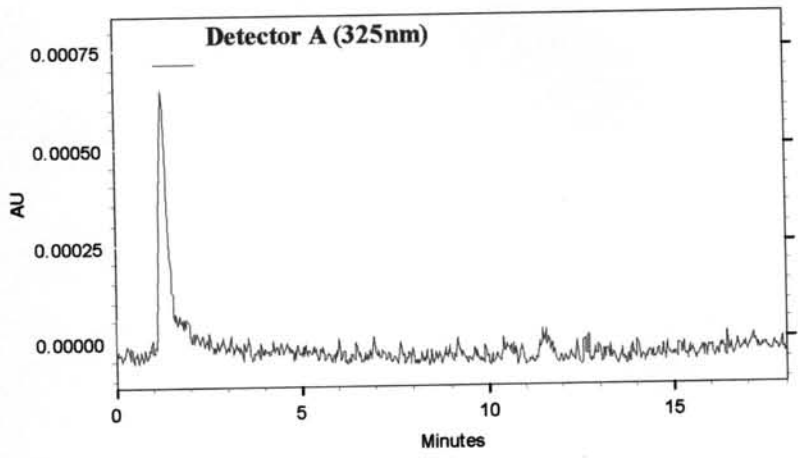

Figure 30 Chromatogram of mobile phase

3.2 Determination of γ-Oryzanol in various production methods of RBO

The content of γ-Oryzanol in various production methods were quantified by HPLC. The analytical results were shown in Figure 31.

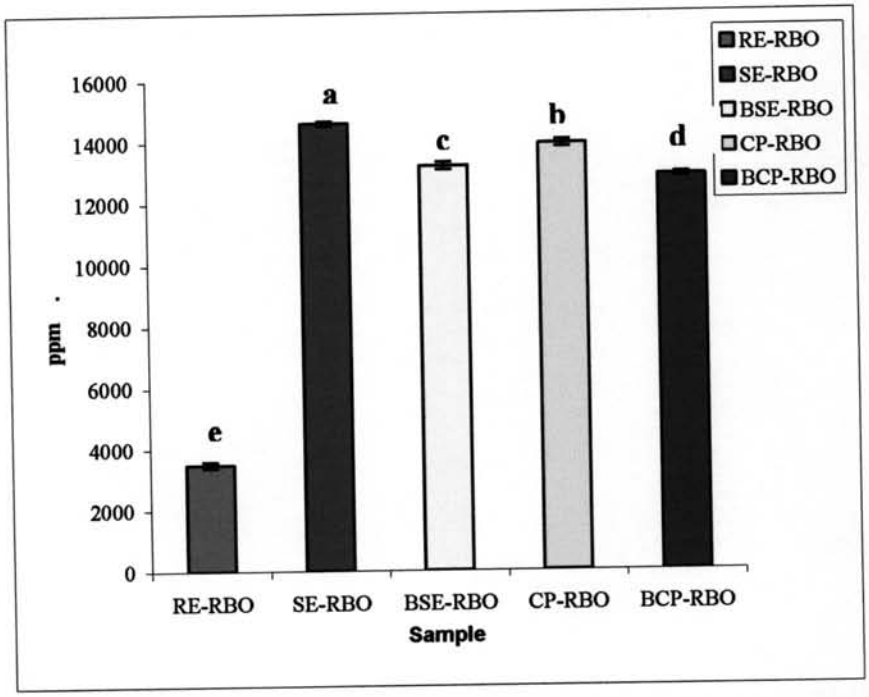

Figure 31 γ-oryzanol contents in various production methods of RBO (Each bar represent mean ± SD, n = 3, a, b,…e = significant difference between group (P<0.05))

Figure 31 showed γ-oryzanol levels across processing steps. SE-RBO gave the highest oryzanol content of 14614.37±70.69 ppm. BSE-RBO gave 13199.41±120.57 ppm. CP-RBO gave 13917.92±115.44 ppm. BCP-RBO gave 12855.82±7.02 ppm and the RE-RBO gave the lowest oryzanol content of 3487.03±100.02 ppm.

The difference in γ-oryzanol content for the different production methods was significant ($P<0.05$). This would tend to indicate that processing steps were affected to γ-oryzanol content in RBO whilst, γ-oryzanol content in RE-RBO was removed more than 70 % when compared with SE-RBO.

3.3 Determination of Vitamin E (α-Tocopherol) in various production methods of RBO

The standard curve of α-tocopherol preparations was carried out in triplicate at each concentration. Then, the prepared working standard solutions were analyzed by HPLC. The peak area and stand curve were shown in Table 14 and Figure 32.

Table 14 Peak area of standard α-tocopherol (standard curve)

Sample	Conc. (μg/mL)	Peak Area
		α-tocopherol
Std 1	4	34750.33
Std 2	8	75523.00
Std 3	16	152444.70
Std 4	40	410375.70

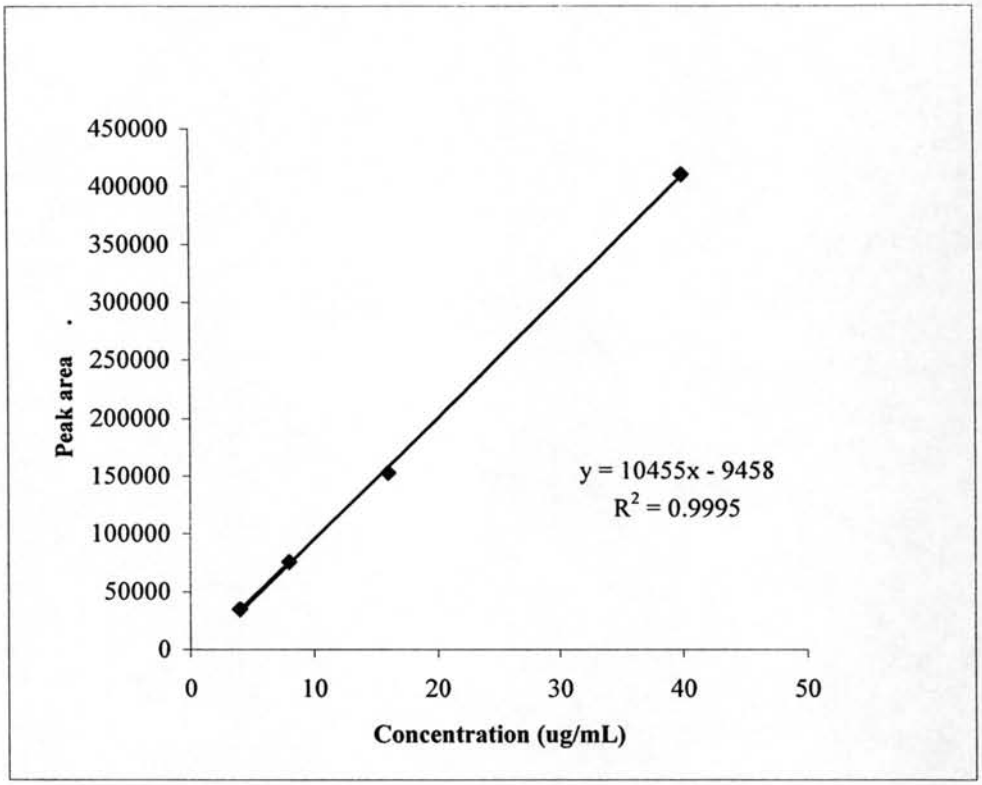

Figure 32 Standard curve of vitamin E (α-tocopherol)

The content of Vitamin E (α-Tocopherol) in various production methods RBO were quantified by HPLC. The analytical results were shown in Figure 33.

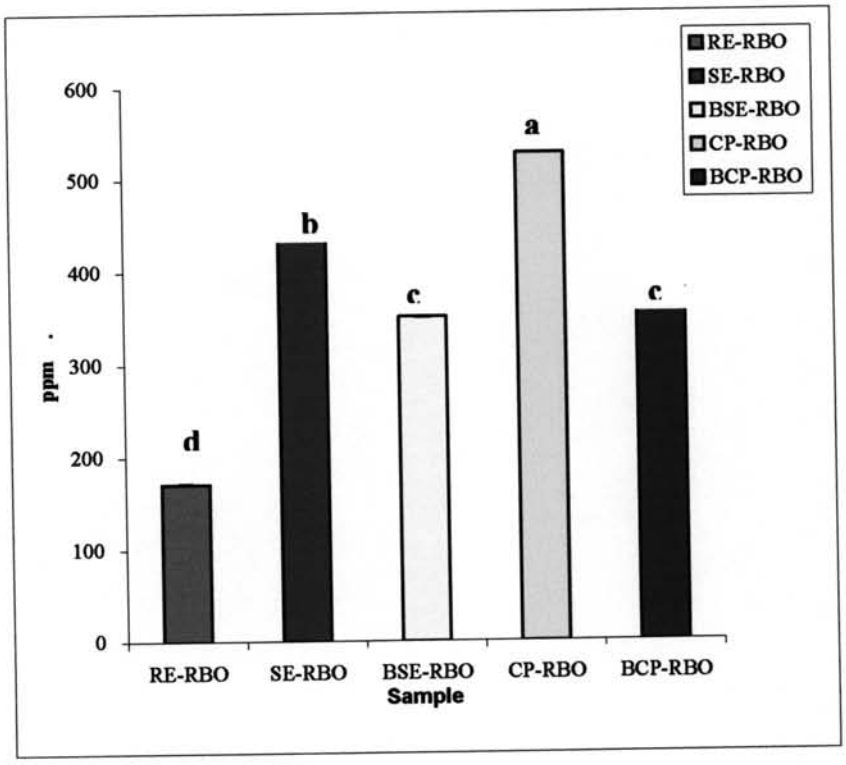

Figure 33 α-tocopherol content in various production methods of RBO
(Each bar represent mean ± SD, n = 3, a, b,...d = significant difference between group (P<0.05))

Figure 33 showed the measured levels of α-tocopherols from the different processing steps in RBO. CP-RBO gave the highest α-tocopherols content at 527.83±0.26 ppm. SE-RBO gave 442.83±0.23 ppm. BCP-RBO gave 357.57±0.38 BSE-RBO gave 350.94±0.38 ppm and the RE-RBO gave the lowest tocopherols content of 170.56±0.31 ppm.

A difference in α-tocopherol levels across some processing steps were significant for SE-RBO, BSE-RBO, CP-RBO, BCP-RBO, and RE-RBO except BSE-RBO and BCP-RBO were not significant (P>0.05). These results indicated that the bleaching step was affected to α-tocopherol content in RBO. α-tocopherol contents were removed by bleaching process about 20-30% and the approximately 80 % α-tocopherols and γ-oryzanol contents were removed in refining process of RBO. In agreement with Marshall (1994), referring to the processing of rice bran oil causes significant variation in the levels of unsaponifiables present in RBO.

Additionally, Table 15 presented the γ-oryzanol content in RE-RBO which was 20.4-fold greater than α-tocopherols. Likewise, the γ-oryzanol content was 33.0, 37.6, and 26.3, 35.9-fold greater than α-tocopherols in SE-RBO, BSE-RBO, CP-RBO and BCP-RBO, respectively.

Table 15 Comparison between tocopherols and oryzanol content

Sample	γ-oryzanol (ppm)	Tocopherol (ppm)	Ratio
RE-RBO	3487.03	170.56	20.44
SE-RBO	14614.37	442.83	33.00
BSE-RBO	13199.41	350.94	37.61
CP-RBO	13917.92	527.83	26.36
BCP-RBO	12855.82	357.57	35.90

From these observations, it was evident that solvent extraction method and cold-pressed method in the production of RBO could be preserved the active components in RBO. Cosmetics material used of these valuable components should ensure maximum recovery of these active components.

4. Oxidative Stability of RBO from Various Production Methods

The estimated oxidative stability can be ranked from the lowest to highest, as follows: BSE-RBO (0.48 h ±0.072), BCP-RBO (2.86 h ± 0.16), RE-RBO (3.69 h ± 0.05), CP-RBO (9.39 h ±1.07), and SE-RBO (9.93 h ± 0.21). Figure 34 showed that the induction times decrease with bleaching step in BSE-RBO and BCP-RBO.

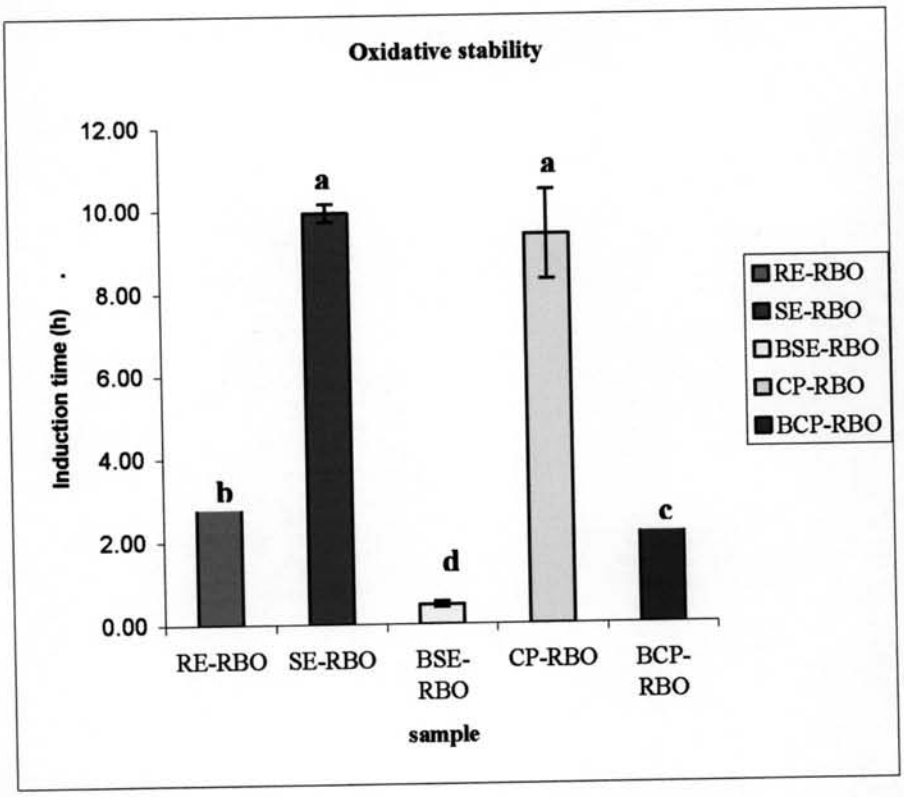

Figure 34 The induction time of various RBO at 120 °C
(Each bar represent mean ± SD, n = 3, a, b,...d = significant difference between group (P<0.05))

The decrease of antioxidant level in RBO resulted in decreases of induction time. These results were consistent with a previous study (Rogers et al., 1993) in that RBO showed good oxidative stability due to the significant levels of nature antioxidants such as γ-oryzanol, α-tocopherols and tocotrienols except RE-RBO had induction time higher than BSE-RBO and BCP-RBO. In other hand, the content of γ-oryzanol and α-tocopherols in RE-RBO were lower than BSE-RBO and BCP-RBO but the induction time was higher than BSE-RBO and BCP-RBO due to content of FFA in RE-RBO was removed during refining steps resulted in reduced of FFA oxidation deterioration.

The difference in induction time for the RBO from various production methods was significant ($P<0.05$). This would tend to indicate that processing steps were affected to oxidative stability of RBO.

5. Kinetics Stability of γ-Oryzanol in Various production methods of RBO

The concentration of γ-oryzanol in rice bran oil decreased as the storage time increased for all accelerated temperature studied. The results suggested that first-order kinetics model could be applied to approximately describe the degradation reaction of the γ-oryzanol in RBO. The first-order degradation kinetics was presented as equation 9.

$$\ln C = \ln Co - kt \quad \text{.....(9)}$$

Where C_0 and C are concentrations of γ-oryzanol at the beginning of reaction and after incubating time t at a given temperature, respectively, k is the first-order rate constant (day^{-1}), and t is the time (day).

The stability of γ-oryzanol was determined by accelerated stability testing method at 40, 60, 70 °C. Plotting the logarithm of rate constants of the reaction against reciprocal of the absolute temperature showed that the temperature dependence of degradation rate constant obeyed Arrhenius equation. All plots were found to be linear, indicating first-order reaction with respect to γ-oryzanol concentration. From slopes of the curves obtained by least squares method, it is possible to calculate k, which indicates the rate constants of γ-oryzanol degradation. The temperature effects on degradation rate of RE- RBO were shown in Figures 35-37 and observed rate constant (k) for γ-oryzanol degradation in RE-RBO during storage at various temperatures were shown in Table 16.

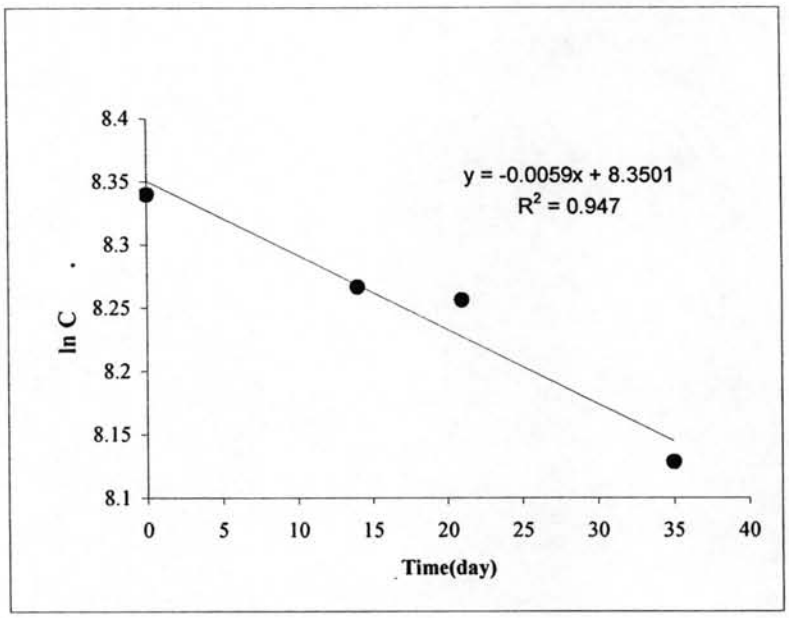

Figure 35 A plot of lnC of γ-oryzanol in RE-RBO versus time at temperature 40°C for a first order reaction

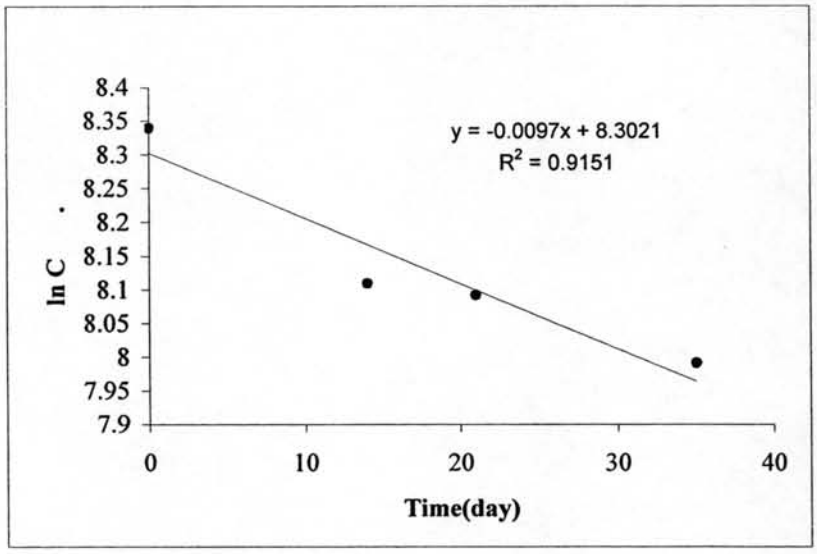

Figure 36 A plot of lnC of γ-oryzanol in RE-RBO versus time at temperature 60°C for a first order reaction

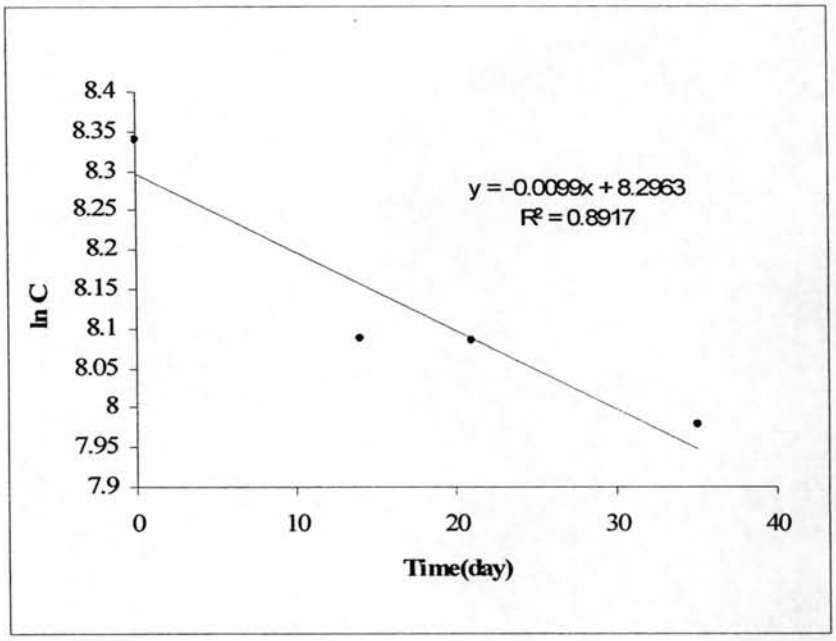

Figure 37 A plot of lnC of γ-oryzanol in RE-RBO versus time at temperature 70°C for a first order reaction

Table 16 Observed rate constants (k) for γ-oryzanol degradation in RE-RBO during storage at various temperatures

Temperature(°C)	k(day^{-1})	S.D.	R^2
40	0.0058	0.0011	0.9449
60	0.0096	0.0005	0.9142
70	0.0099	0.0001	0.8916

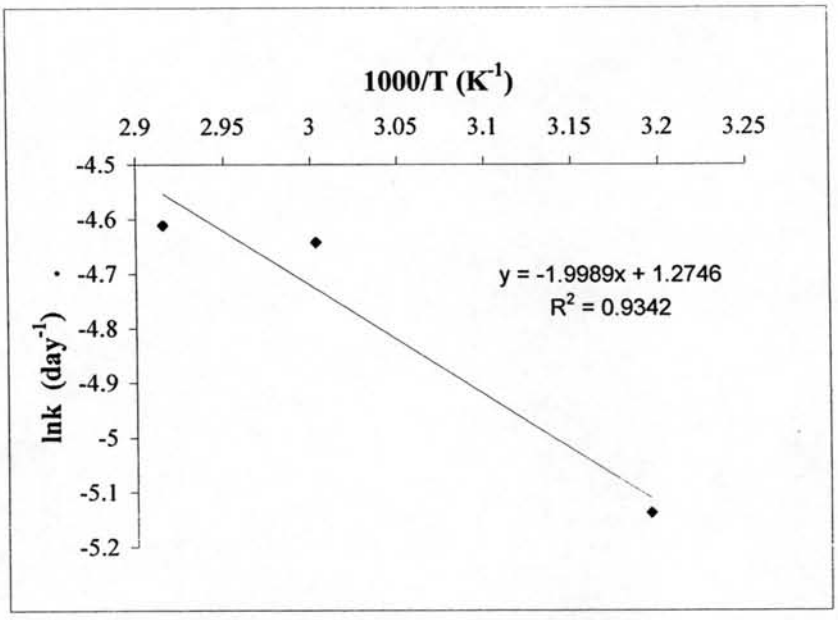

Figure 38 Arrhenius plot for the first-order rate constant of γ-oryzanol degradation in RE-RBO over the temperature range of 40-70 °C

Plotting the logarithm of rate constants of the reaction (ln k) against reciprocal of the absolute temperature (1000/T) (Figure 38) showed that the temperature dependence of degradation rate constant obeyed Arrhenius relationship :

$$\ln k = \ln k_0 - Ea / RT \text{.....(10)}$$

Where k is the reaction rate constant (day^{-1}), k_0 is the pre-exponential constant (day^{-1}); Ea is the activation energy (cal/mol); R is the universal gas constant (1.987 calories $degree^{-1}$ $mole^{-1}$) and T is the absolute temperature (K). Using equation 10, the heat of activation, Ea, was calculated from the slope of the straight line obtained by least squares. The Ea value for γ-oryzanol degradation in RE-RBO was 3.97 kcal / mol.

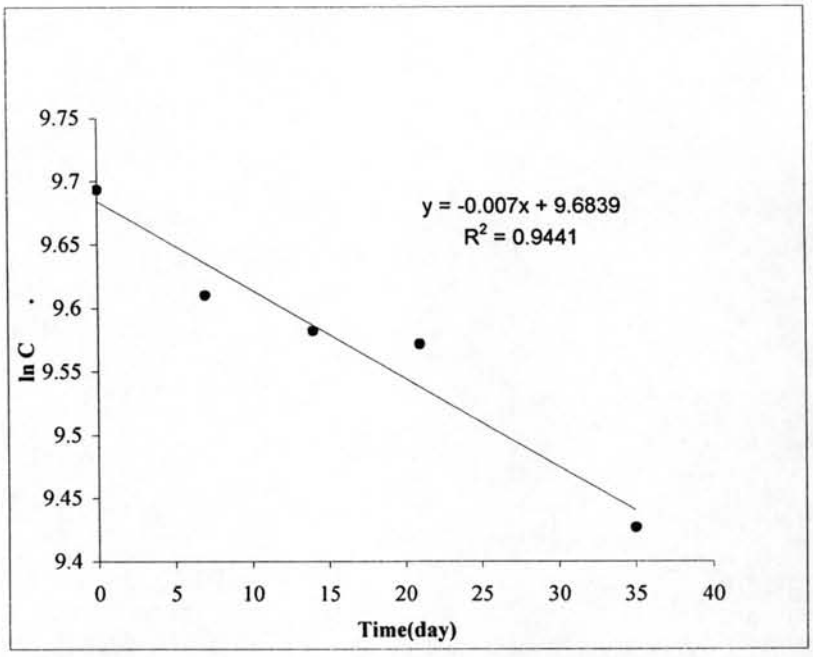

Figure 39 A plot of lnC of γ-oryzanol in SE-RBO versus time at temperature 40 °C for a first order reaction

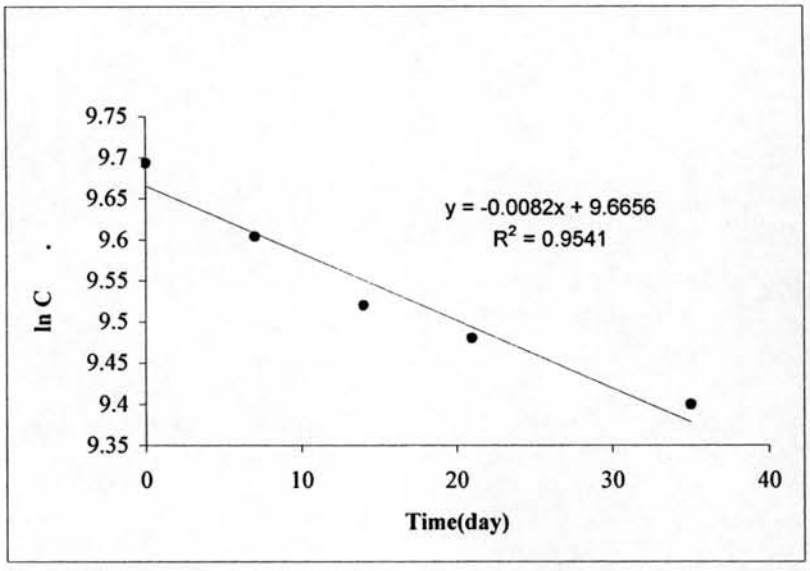

Figure 40 A plot of lnC of γ-oryzanol in SE-RBO versus time at temperature 60 °C for a first order reaction

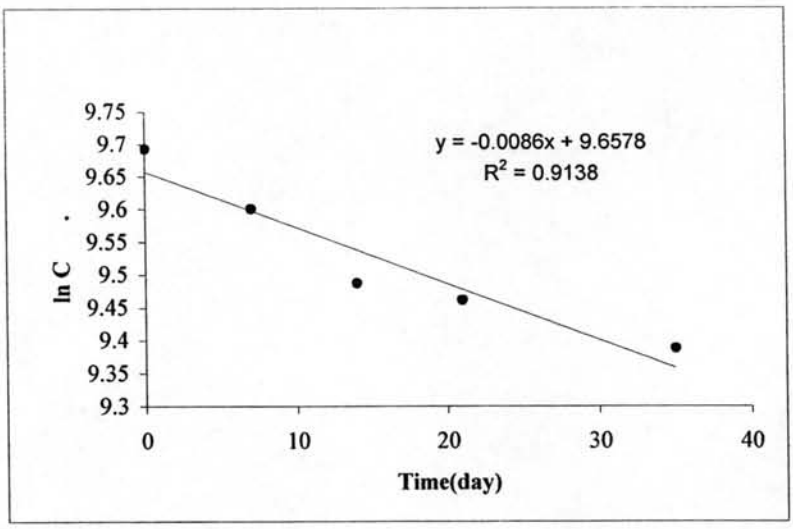

Figure 41 A plot of lnC of γ-oryzanol in SE-RBO versus time at temperature 70 °C for a first order reaction

Table 17 Observed rate constants (k) for γ-oryzanol degradation in SE-RBO during storage at various temperatures

Temperature(°C)	k(day^{-1})	S.D.	R^2
40	0.0056	0.0002	0.9429
60	0.0103	0.0006	0.9542
70	0.0116	0.0003	0.9078

The Ea value for γ-oryzanol degradation in SE-RBO was 5.35 kcal/mol.

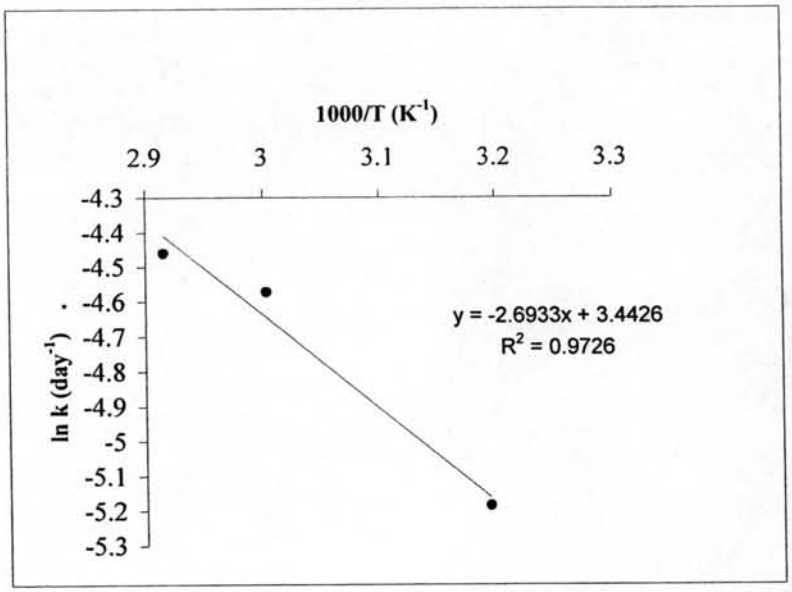

Figure 42 Arrhenius plot for the first-order rate constant of γ-oryzanol degradation in SE-RBO over the temperature range of 40-70 °C

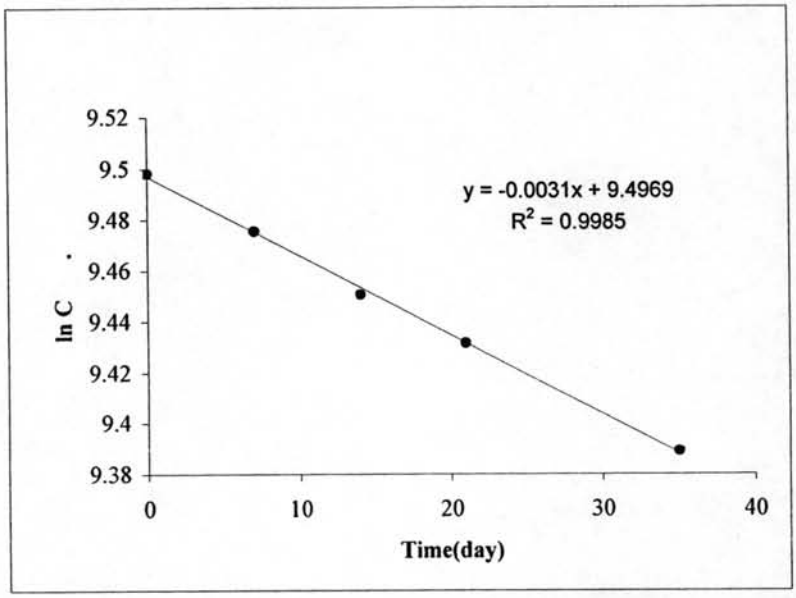

Figure 43 A plot of lnC of γ-oryzanol in BSE-RBO versus time at temperature 40 °C for a first order reaction

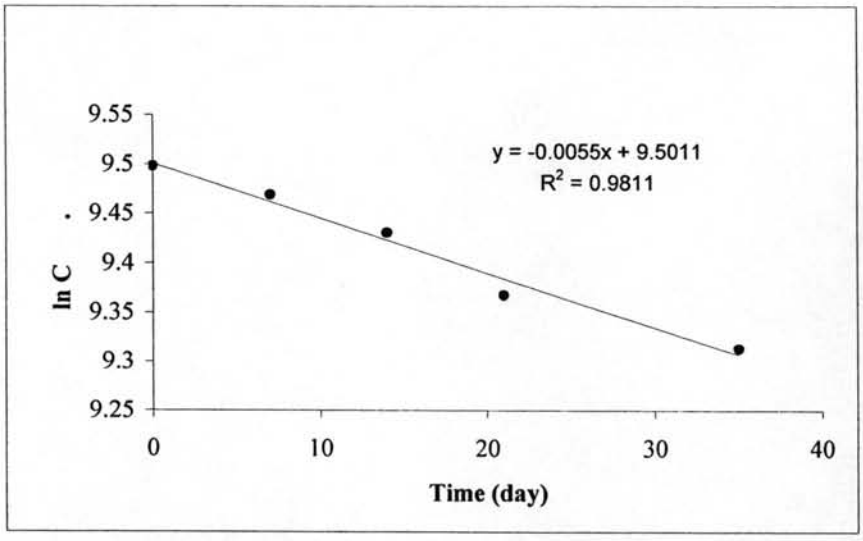

Figure 44 A plot of lnC of γ-oryzanol in BSE-RBO versus time at temperature 60 °C for a first order reaction

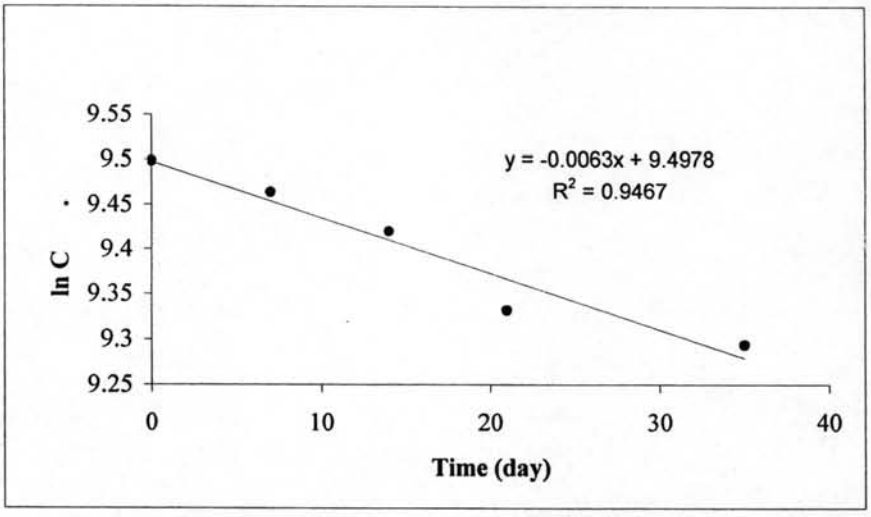

Figure 45 A plot of lnC of γ-oryzanol in BSE-RBO versus time at temperature 70 °C for a first order reaction

Table 18 Observed rate constants (k) γ-oryzanol degradation in BSE-RBO during storage at various temperatures.

Temperature(°C)	k(day^{-1})	S.D.	R^2
40	0.0031	0.0004	0.9785
60	0.0056	0.0007	0.9672
70	0.0063	0.0004	0.9539

The Ea value for γ-oryzanol degradation in BSE-RBO was 5.09 kcal / mol

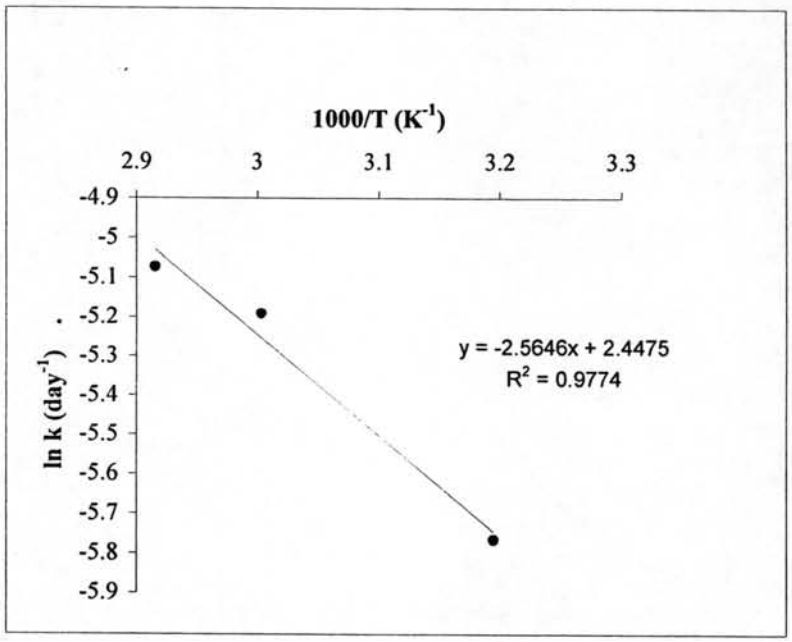

Figure 46 Arrhenius plot for the first-order rate constant of γ-oryzanol degradation in BSE-RBO over the temperature range of 40-70 °C

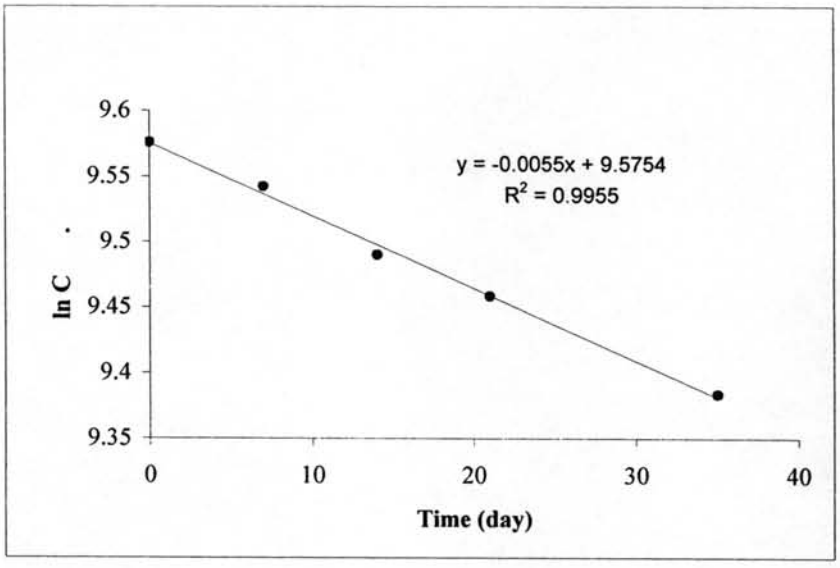

Figure 47 A plot of lnC of γ-oryzanol in CP-RBO versus time at temperature 40 °C for a first order reaction

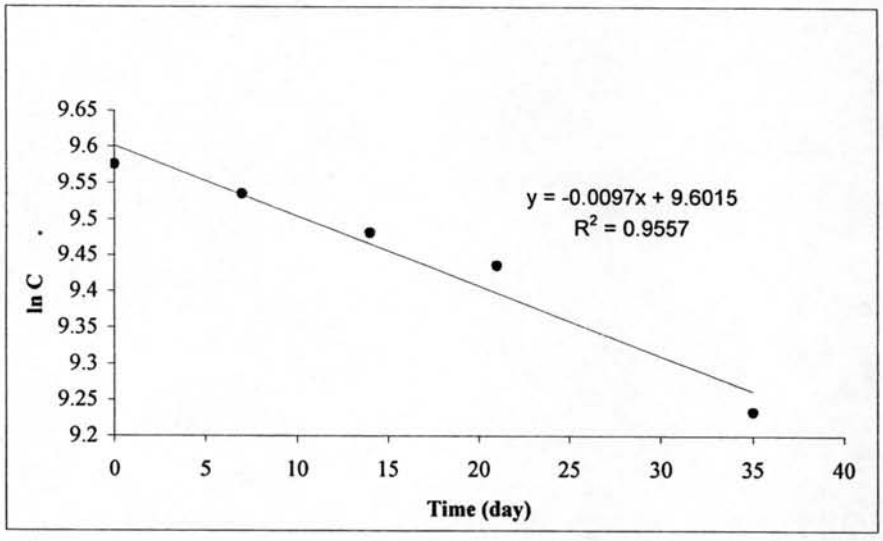

Figure 48 A plot of lnC of γ-oryzanol in CP-RBO versus time at temperature 60 °C for a first order reaction

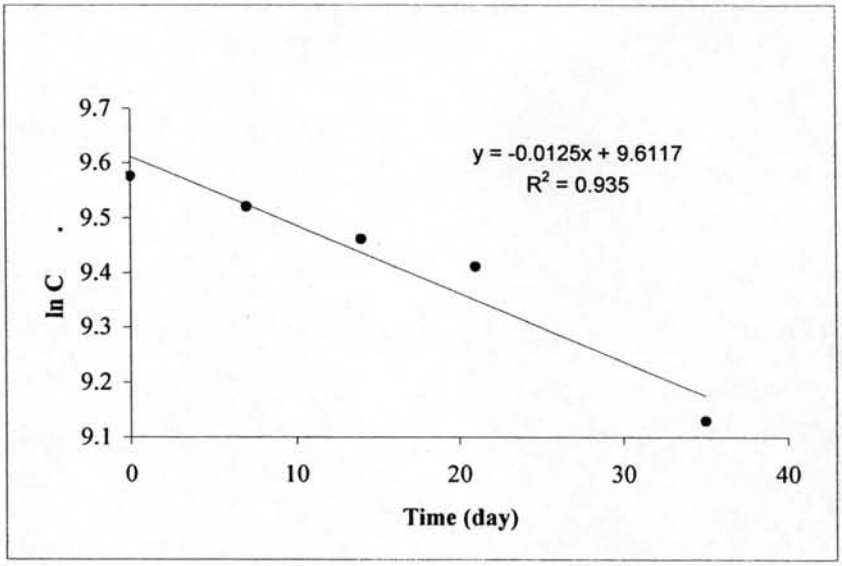

Figure 49 A plot of lnC of γ-oryzanol in CP-RBO versus time at temperature 70 °C for a first order reaction

Table 19 Observed rate constants (k) for γ-oryzanol degradation in CP-RBO during storage at various temperatures

Temperature(°C)	k(day^{-1})	S.D.	R^2
40	0.0055	0.0004	0.9926
60	0.0097	0.0005	0.9557
70	0.0125	0.0003	0.9349

The Ea value for γ-oryzanol degradation in CP-RBO was 5.80 kcal / mol

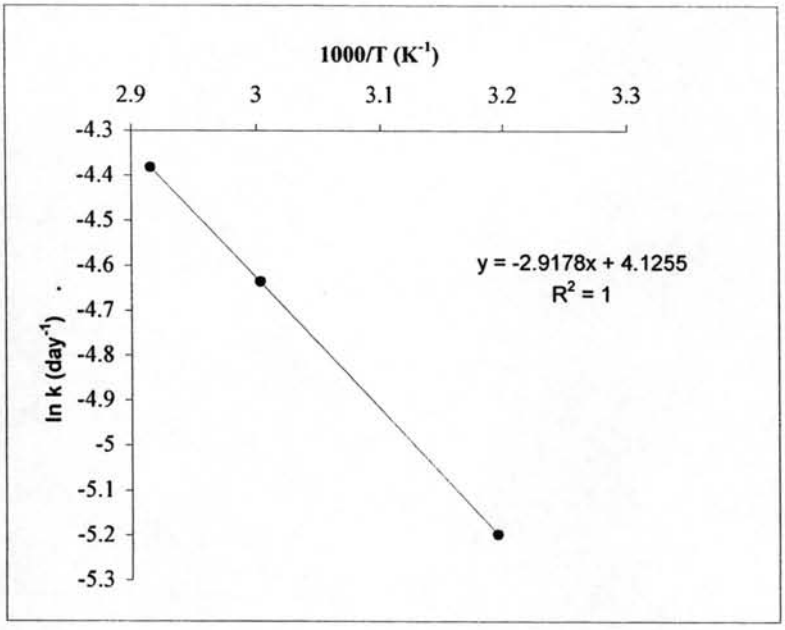

Figure 50 Arrhenius plot for the first-order rate constant of γ-oryzanol degradation in CP-RBO over the temperature range of 40-70 °C

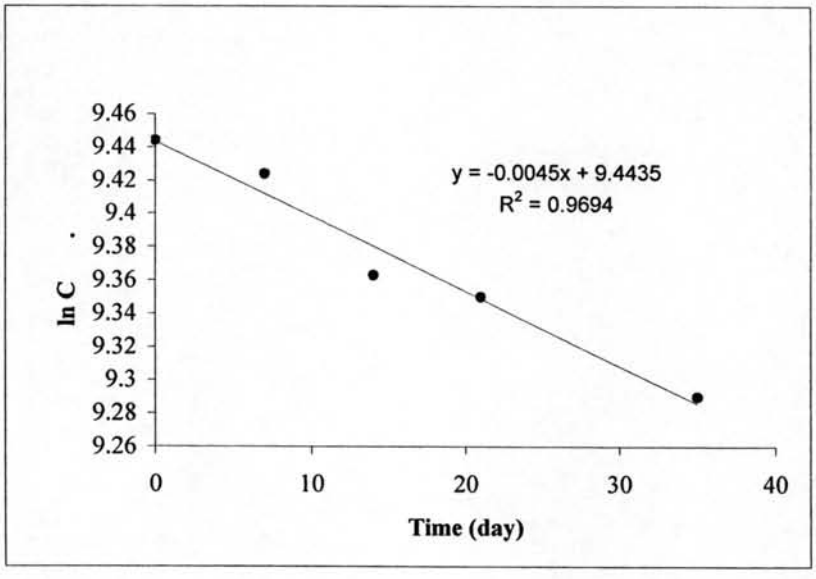

Figure 51 A plot of lnC of γ-oryzanol in BCP-RBO versus time at temperature 40 °C for a first order reaction

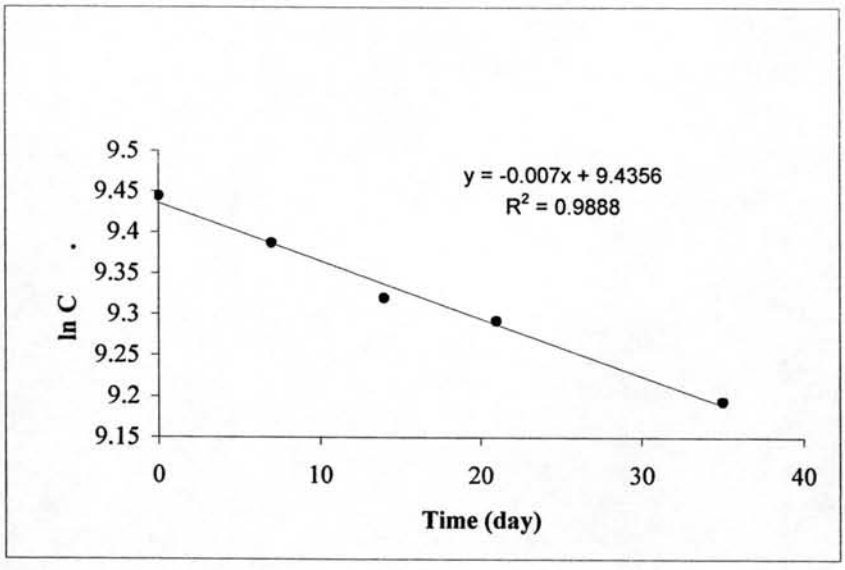

Figure 52 A plot of lnC of γ-oryzanol in BCP-RBO versus time at temperature 60 °C for a first order reaction

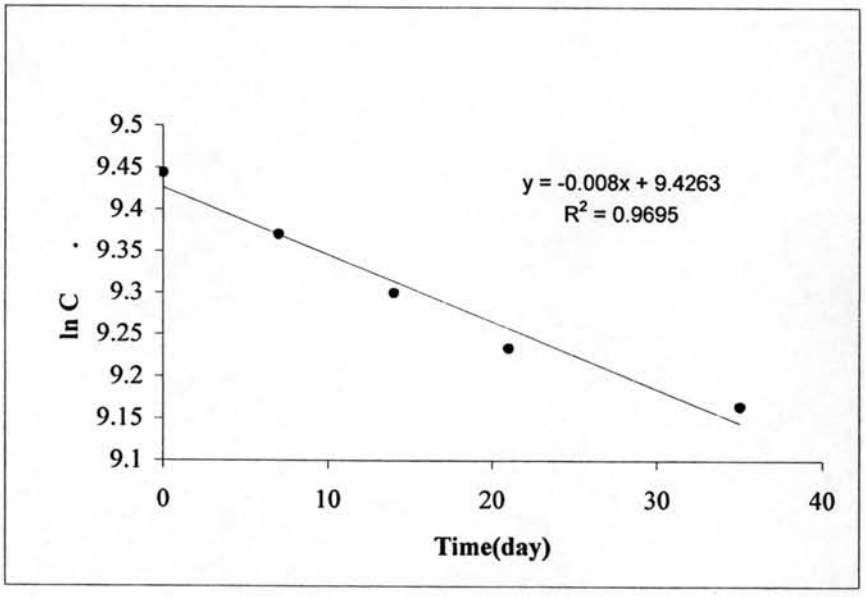

Figure 53 A plot of lnC of γ-oryzanol in BCP-RBO versus time at temperature 70 °C for a first order reaction

Table 20 Observed rate constants (k) for γ-oryzanol degradation in BCP-RBO during storage at various temperatures

Temperature(°C)	k(day^{-1})	S.D.	R^2
40	0.0045	0.0006	0.9601
60	0.0070	0.0002	0.9817
70	0.0080	0.0003	0.9625

The Ea value for γ-oryzanol degradation in BCP-RBO was 4.20 kcal / mol.

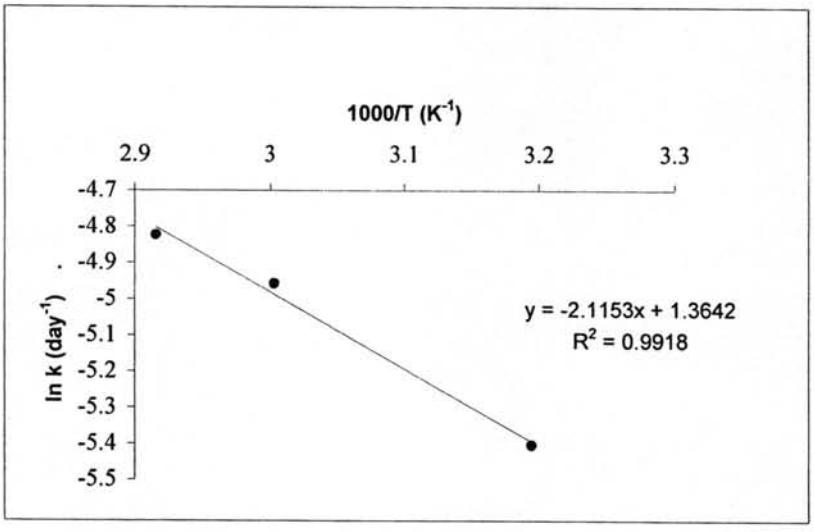

Figure 54 Arrhenius plot for the first-order rate constant of γ-oryzanol degradation in BCP-RBO over the temperature range of 40-70 °C

Table 21 Activated Energy of RBO from various production methods

Sample	Slope	R^2	Ea (kcal/mol)
RE-RBO	2.00	0.9342	3.97
SE-RBO	2.69	0.9726	5.35
BSE-RBO	2.56	0.9774	5.09
CP-RBO	2.92	1.0000	5.80
BCP-RBO	2.11	0.9918	4.20

Activated Energy of RBO from various production methods was shown in Table 21. The linear nature of Arrhenius plot was excellent verification of the methods utility in prediction of degradation rate under a different range of temperatures (Bibart, 1979; Garrett and Carper, 1955). The predicted degradation rate (k) can be used to determine half-life ($t_{1/2}$) of the products following equation 11.

The difference in activated energy for the different production methods was significant ($P<0.05$). This would tend to indicate that processing steps were affected to activate energy in various RBO.

$$t_{1/2} = 0.693/k \quad \text{..... (11)}$$

Where k is the first-order rate constant.

Table 22 The predicted degradation rate constant (k) and half-life ($t_{1/2}$) of γ-oryzanol content in RBO at room temperature (32 ± 2 °C)

Sample	k x 1000 (day^{-1})	Half-life(day)
RE-RBO	5.09	136.14
SE-RBO	4.56	151.97
BSE-RBO	2.58	268.60
CP-RBO	4.34	159.67
BCP-RBO	3.81	181.90

The concentration of γ-oryzanol in RBO decreased as the storage time increased for all accelerated temperature studied. In order to determine the order of rate law, observed data were fitted with zero, first and second order equations. Fitting with first order equation showed the highest linear correlation coefficient (R^2). This indicated that degradation of γ-oryzanol followed first order rate law. The results suggested that first-order kinetics model could be applied to describe the degradation reaction of the γ-oryzanol in RBO from various production methods. The temperature effects on degradation rate of each RBO were shown in Table 16-20. Increasing the

heating temperature from 40°C to 70°C resulted in increased rate of degradation (k) of γ-oryzanol in RBO about 2 times. The main reaction that caused degradation of γ-oryzanol could be the oxidation of the compound by oxidation products of RBO which formed during the thermal treatment.

Table 22 showed the predicted values of rate constants and half-life at room temperature (32 ± 2°C).The results showed that the rate constant of bleaching RBOs were lower than non bleaching RBO. These results indicated that bleaching process that reduced γ-oryzanol content could be prolonged half-life of RBO. The study confirmed that when activated bleaching clays were added to the oil it removed pigments, oxidized lipids and polar components from the oil (Marshall, 1994). But, the RE-RBO exhibited the lowest half-life of γ-oryzanol. This result was consistent with the previous study in that SE, BSE, CP and BCP gave excellent oxidative stability due to its high content of γ-oryzanol and α-tocopherols. RE-RBO presented lower stability due to the removal approximately 70-80 % of antioxidant components.

6. Formulation of Oil-in-Water Emulsions from Various production methods of RBO

6.1 Preparation of Various RBO Emulsions

Emulsions were prepared according to Table 5. The physical appearances of various RBO were shown in Figure 55. RE-RBO gave white emulsions. CP-RBO emulsions gave less color yellow than SE-RBO emulsions. BCP-RBO emulsions gave less yellow color when compare to CP-RBO emulsions. Also, the BSE-RBO emulsions gave less yellow color than SE-RBO emulsions.

Figure 55 Physical appearances of emulsions from various RBO

6.2 Determination of Physical Properties

6.2.1 Determination of pH

The estimated pH can be ranked from the lowest to highest, as follows: BSE-RBO (5.17 ±0.0153), RE-RBO (5.23 ± 0.0200), BCP-RBO (5.27 ± 0.0252), CP-RBO (5.41±0.0100), and SE-RBO (5.43 ± 0.0058). Figure 56 showed that pH decrease with bleaching step in BSE-RBO and BCP-RBO. Due to the decrease of antioxidant level in RBO resulted in increases of FFA.

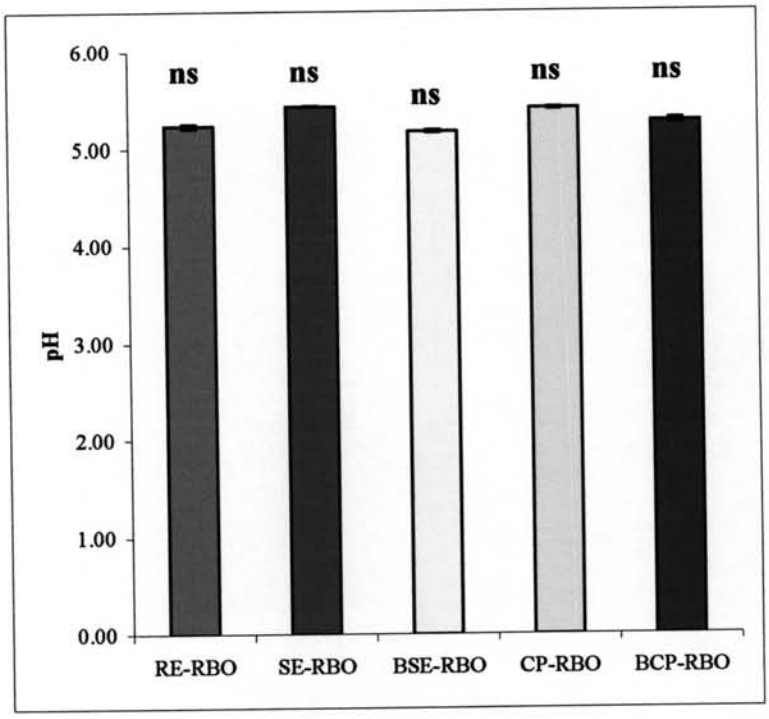

Figure 56 pHs of emulsions from various RBO
(Each bar represent mean ± SD, ns = no significant difference between group (P>0.05))

The difference in term of pH for the RBO from various production methods were not significant (P>0.05) for RE-RBO and BCP-RBO emulsions, and CP-RBO and SE-RBO emulsions. The result showed pHs of all various RBO formulations were approximately in an acceptable range of skin pH (5-6).

6.2.2 Determination of Viscosity

The estimated viscosity can be ranked from the lowest to highest, as follows: SE-RBO (4262.68 ± 76.91), BSE-RBO (4427.14 ± 40.36), CP-RBO (4900.07 ± 44.69), BCP-RBO (5104.95 ± 92.49), and RE-RBO (5365.59 ± 70.30). Figure 57 showed that the viscosities were increased with processing steps in RBO were increased.

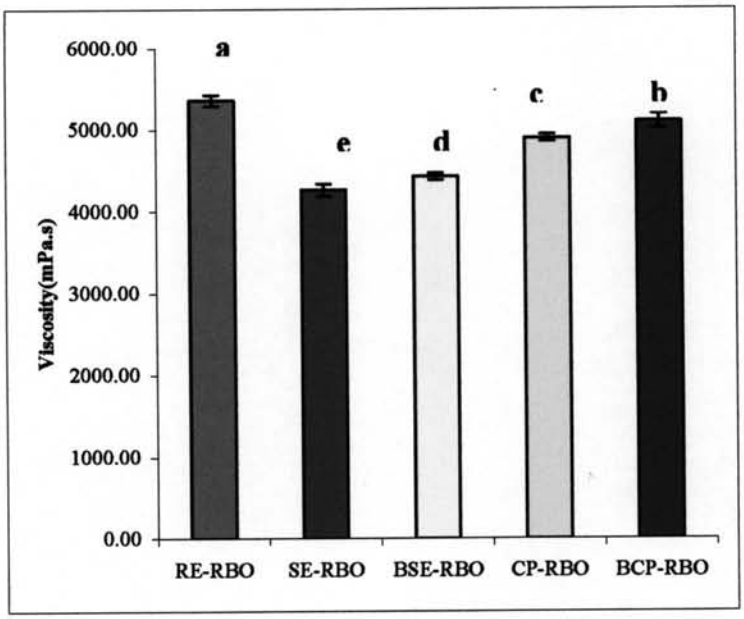

Figure 57 Viscosities of emulsions from various RBO
(Each bar represent mean ± SD, n = 3, a, b,...d = significant difference between group (P<0.05))

The difference in viscosities for the RBO from various production methods was significant (P<0.05). This would tend to indicate that processing steps were affected to viscosity of RBO emulsions.

6.3 Sensory Evaluation of RBO Formulations from Various Production Methods

The color, odor, skin feel, smooth cream mass and spreadability were evaluated by the panelists (n=15). The feelings were ranked at the end of study in 1 to 5 scales of satisfaction: 1 as 'least', 2 as 'slight', 3 as 'moderate', 4 as 'considerable', and 5 as 'most'. The mean score of satisfactory feelings were shown in Figure 58 the details of the feelings were evaluated.

Figure 58 illustrated the mean score of RBO formulations from various production methods. RE-RBO was evaluated as the most 'satisfy' with its color and spreadability. CP-RBO was evaluated as the most 'satisfy' with skin feel and BCP-

RBO was evaluated as the most 'satisfy' with odor and smooth cream mass. On the other hand, SE-RBO got the least score in all categories.

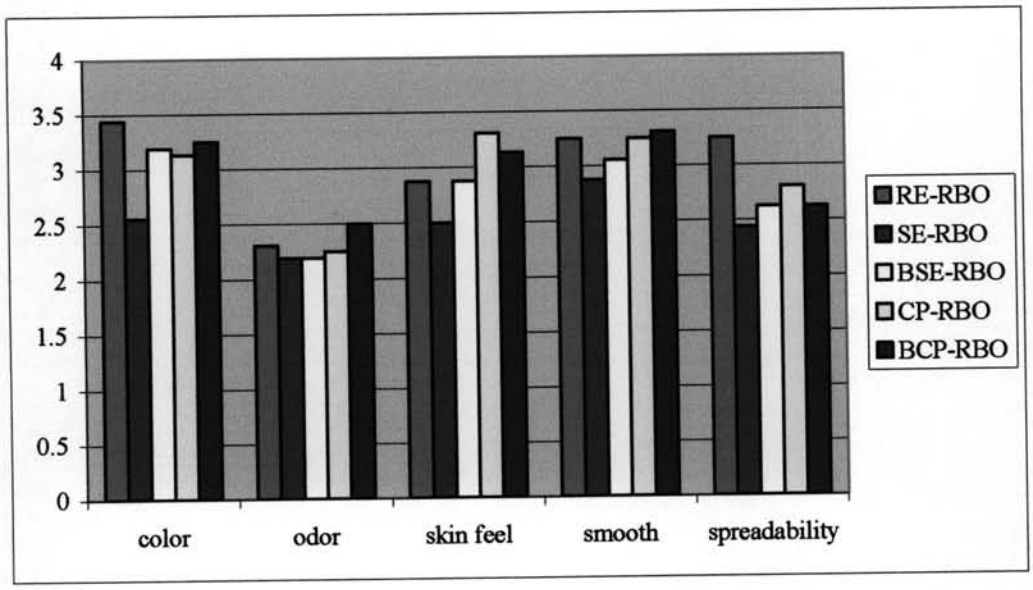

Figure 58 Mean score of satisfactory feel evaluation by the panelists

6.4 Physical Stability Testing

The product should pass six cycles of temperature testing at 4 °C and 45 °C. The results showed that all formula showed good stability after 6 cycles of temperature cycling.

6.4.1 pH of Oil-in-Water RBO Emulsions

The pH values of RBO emulsions are shown in Figure 59.

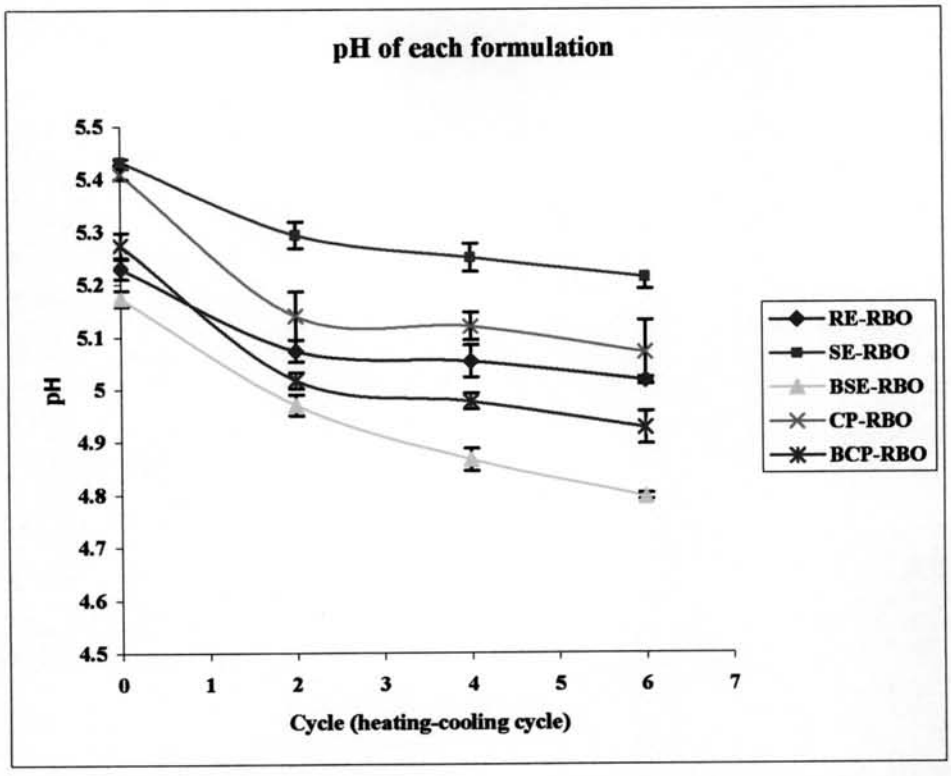

Figure 59 pHs of various RBO emulsions during heating-cooling cycle

The pH of all preparations were approximately 5.30 before temperature cycling. Figure 59 showed that during temperature cycling the pH of all formulations slowly decreased with time to acidic pH. The lowest pH, 4.80 ± 0.068, was found in formulation BSE-RBO. It was possibly due to the hydrolysis of some lipid in the emulsions leading to the formation of free fatty acid which gradually reduced the pH of the system (Hansrani, Davis and Groves, 1983; Herman and Groves, 1992).

Differences in physical stability testing in term pH of oil-in-water emulsions before and after heating-cooling cycles were significant ($P<0.05$) for all formulation. The results indicated that heating-cooling cycle affected pH in all various RBO emulsions.

6.4.2 Viscosity of Oil-in-Water RBO Emulsions

Figure 60 showed the apparent viscosity of various RBO during temperature cycling.

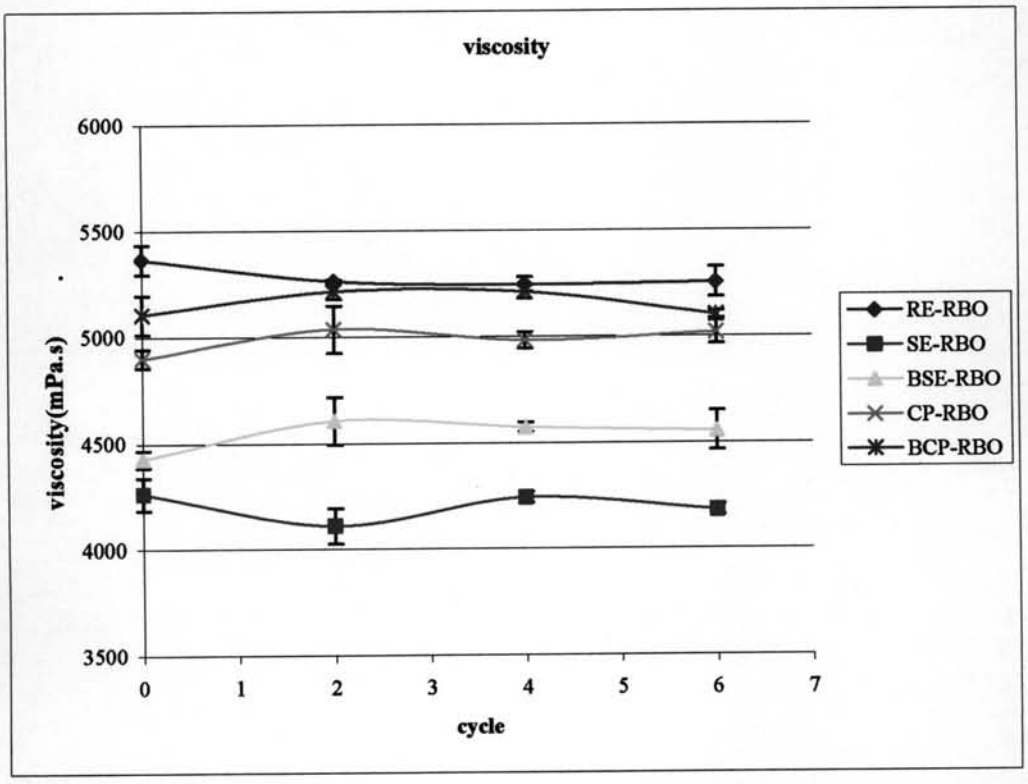

Figure 60 Viscosities of various RBO emulsions during heating-cooling cycle

The apparent viscosity of RE-RBO was 5365.87 ± 70.30 at cycle 0. The apparent viscosity of RE-RBO decreased to 5261.41 ± 7.71 at cycle 2, and after that a slow changing of apparent viscosity was observed until completion of temperature cycling.

The apparent viscosity of SE-RBO was 4262.68 ± 76.91 at cycle 0.After that, the apparent viscosity was decreased to 4109.71 ± 83.24 at cycle 2 and then small changing of viscosity was increased to 4182.84 ± 25.72 until complete temperature cycling.

The apparent viscosity of BSE-RBO was 4427.14 ± 40.36 at cycle 0.After that, the apparent viscosity was increased to 4606.09 ± 112.06 at cycle 2 and then small changing of viscosity was decreased to 4556.65 ± 92.81 until complete temperature cycling.

The apparent viscosity of CP-RBO was 4900.07 ± 44.69 at cycle 0.After that, the apparent viscosity was increased to 5035.92 ± 110.79 at cycle 2 and then small changing was decreased to 5018.49 ± 54.33 until complete temperature cycling.

The apparent viscosity of BCP-RBO was 5104.95 ± 92.49 at cycle 0.After that, the apparent viscosity was increased to 5213.65 ± 36.66 at cycle 2 and the small changing was decreased to 5100.97 ± 18.62 until complete temperature cycling.

Differences in physical stability testing in term viscosity of oil-in-water emulsions before and after heating-cooling cycles were not significant ($P>0.05$) for all formulation. The results indicated that heating-cooling cycle did not affected to physical stability in term viscosity in all various RBO emulsions.